PCCP

Accepted Manuscript

ROYAL SOCIETY OF CHEMISTRY

www.rsc.org/pccp

Rate coefficient for the reaction of OH radicals with cis-3-hexene: an experimental-theoretical study

Thaís da Silva Barbosa [a], Silvina Peirone[b], Javier A. Barrera[b], Juan P. A. Abrate[b], Silvia I. Lane [b], Graciela Arbilla[c] and Glauco Favilla Bauerfeldt [a,*].

a. Departamento de Química. Instituto de Ciências Exatas. Universidade Federal Rural do Rio de Janeiro. Seropédica, RJ, Brazil. Fax: +55 21 2682 2807; Tel: +55 21 2682 2807. bauerfeldt@ufrrj.br

b. Instituto de Investigaciones em Fisicoquímica de Córdoba (INFIQC), CONICET, Centro Láser de Ciencias Moleculares, Departamento de Fisicoquímica, Facultad de Ciencias Químicas, Universidad Nacional de Córdoba, Ciudad Universitaria, (5000) Córdoba, Argentina. s-lane@fcq.unc.edu.ar

c. Departamento de Físico-Química. Instituto de Química, Universidade Federal do Rio de Janeiro. Rio de Janeiro, RJ, Brazil. Fax: +55 21 25627265; Tel: +55 21 25627755; E-mail: gracielaiq@gmail.com

* Author to whom correspondence should be addressed. Electronic mail: bauerfeldt@ufrrj.br

Abstract

The kinetics of the cis-3-hexene + OH reaction were investigated by experimental relative rate method and at the Density Functional Theory level. The experimental set-up consisted of a 200 L Teflon bag, operated at atmospheric pressure and 298 K. OH radicals were produced by the photolysis of H_2O_2 at 254 nm. Relative rate coefficients were determined by comparing the decays of the cis-3-hexene and reference compounds (cyclohexene, 2-buten-1-ol and allyl ether). The mean second-order rate coefficient value found was (6.27±0.66) × 10^{-11} cm^3 $molecule^{-1}$ s^{-1}, the uncertainty being estimated by propagation of errors. Theoretical calculations for the addition reaction of OH to cis-3-hexene have also been performed, at the BHandHLYP/aug-cc-pVDZ level, in order to investigate the reaction mechanism, to clarify the experimental observations and to model the reaction kinetics. Different conformations of the reactants, pre-barrier complexes and saddle points were considered in our calculations. The individual rate coefficients, calculated for each conformer of the reactant, at 298 K, using a microcanonical variational transition state method, are 4.19 × 10^{-11} and 1.23 × 10^{-10} cm^3 $molecule^{-1}$ s^{-1}. The global rate coefficient was estimated from the Boltzmann distribution of the conformers as 8.10 × 10^{-11} cm^3 $molecule^{-1}$ s^{-1}, is in agreement with the experimental value. Rate coefficients calculated over the temperature range from 200 – 500 K are also given. Our results suggest that the complex mechanism, explicitly considering different conformations for the stationary points, must be taken into account for a proper description of the reaction kinetics.

Keywords

cis-3-hexene + OH ; rate coefficients; experimental relative rate method; RRKM; OH addition reaction

Graphical and Textual Abstract

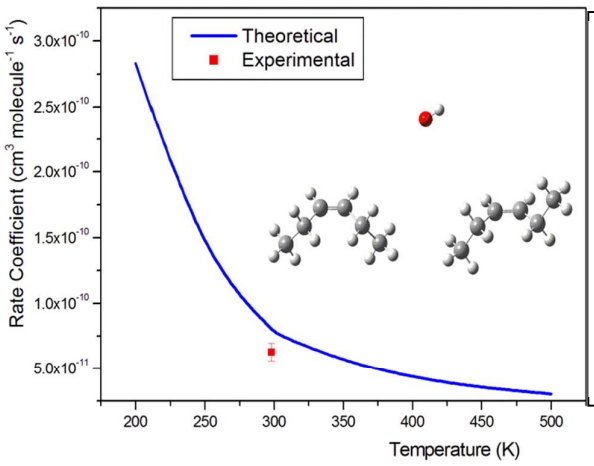

Microcanonical variational rate coefficients and experimental rate coefficients for the OH addition to cis-3-hexene have been determined. Theoretical results showed a non-Arrhenius profile and good agreement with the experimental data.

1. Introduction

Volatile organic compounds (VOCs) are emitted into the atmosphere from biogenic and anthropogenic sources. [1-3] Reactions of VOCs lead to a complex series of chemical transformations, generally resulting in the formation of ozone and secondary organic aerosols.[4] Among the VOCs, unsaturated compounds from anthropogenic sources are most emitted from fossil fuel combustion and industrial processes. In this group, cis-3-hexene is emitted among other unsaturated hydrocarbons in gasoline vapor[5,6] and is the focus of this study.

In the troposphere, cis-3-hexene is expected to be chemically removed by reactions with ozone and hydroxyl and nitrate radicals and rate coefficients for the ozone[7] and nitrate[8] reactions are available. OH radicals are strong oxidizing agents, the major source being through the photolysis of ozone. This reaction yields $O(^1D)$, which further reacts with water vapor and generates OH radicals. Other minor sources include the photolysis of gaseous nitrous acid and hydrogen peroxide. Due to its photolytic sources OH radicals are important oxidants especially during day-light hours. Despite the importance of the OH-initiated processes, no previous experimental investigation concerning the prediction of the rate coefficients for the reaction of OH radicals with cis-3-hexene, to the best of our knowledge, can be found. Using structure-activity relationships, Grosjean and co-workers have determined the rate coefficient for the reaction of cis-3-hexene with OH radicals and the value found was 6.3×10^{-11} cm^3 $molecule^{-1}$ s^{-1}.[9]

Moreover, from a fundamental point of view, our research group has been devoted to the understanding of the reactivity of unsaturated compounds towards OH radicals, with

respect to the reactivity of the alkenes analogues.[10,11] And, in regard to the unsaturated alcohols, cis-3-hexen-1-ol is a very important biogenic VOC, emitted by vegetation.[12,13] Although, accurate values for rate coefficients of the cis-3-hexen-1-ol + OH reaction are already available in the literature,[14-17] rate coefficients for the cis-3-hexene + OH reaction are lacking.

The main goal of this work is the study of the cis-3-hexene + OH reaction kinetics by the experimental relative rate method and computational procedures. The rate coefficient was experimentally obtained at 298 K and atmospheric pressure for the addition reaction of OH radicals to cis-3-hexene. In order to explore the reaction mechanism, a theoretical model was investigated at the Density Functional Theory (DFT) level and Microcanonical Variational Transition State methods.

The proposed mechanism for the OH addition to cis-3-hexene, at atmospheric conditions, follows the general OH addition to unsaturated compounds: a pre-barrier complex (PC) is reversibly formed from the isolated reactants, via a barrierless association path and then reacts, passing through different saddle points, forming the radicals P1 or P2. Literature suggests that two kinds of pre-barrier complexes can be expected: a σ-type, in which the OH radical lies parallel to the plane and a π-type, in which the OH radical lies perpendicularly to the plane that contains the double bond. [18-20] Moreover, the π-type pre-barrier complex was shown to be the most important. [21-23] Therefore, in this work, only the π-type pre-barrier complex (π-PC) was considered. This mechanism for the OH addition to cis-3-hexene is schematized as follows.

cis-3-hexene + OH → π-PC (Reaction 1, k_1)

π-PC → cis-3-hexene + OH (Reaction 2, k_{-1})

π-PC → P_1 (Reaction 3, $k_2^{(1)}$)

π-PC → P_2 (Reaction 4, $k_2^{(2)}$)

In this set of chemical equations, reactions 1 and 2 represent the formation and dissociation of the pre-barrier complex (π-PC), with rate coefficients k_1 and k_{-1}, respectively. The formation of products P1 and P2 are represented by reactions 3 and 4, with rate coefficients $k_2^{(1)}$ and $k_2^{(2)}$, respectively.

For a proper description of the OH radicals with any unsaturated compound, the H abstraction reactions should also be taken into account, and the expected experimental value for the global rate coefficient is the sum of the addition and abstraction rate coefficients. However, since contribution of the abstraction rate coefficient to the global kinetics is expected to be about 10%, this channel has not been included in our calculations.

2. Experimental Section

The experimental work has been conducted at the *Instituto de Investigaciones en Fisicoquímica de Córdoba, Argentina.* The reaction chamber consisted of a 200 L collapsible Teflon bag, inert and transparent to UV radiation, and the rate coefficients were measured by the relative rate method. This methodology has been satisfactorily performed at this laboratory for the study of the kinetics of several other reactions.[24-26]

The reactant and the reference compound were carried into the chamber using ultrapure air. Five germicide lamps (Philips 30W), with a λ maximum around 254 nm, were used to promote photolysis of the OH precursor in a controlled fashion. In this work, H_2O_2 was used and was introduced into the reaction chamber using a syringe in excess quantity. Photolysis time varied from 10 seconds to 1 minute. Samples were periodically collected using a calibrated gas syringe (Hamilton *gas tight* 5 mL), and immediately injected in a gas chromatograph (Clarus 500–PerkinElmer) equipped with an Elite-1 column (Perkin-Elmer, length: 30 m, inner diameter 0.32 mm, film thickness: 0.25 μm) and a flame detector. The carrier gas helium with flow rate of 0.8 mL min^{-1} was used. Measurements were carried out in the splitless mode. The temperature of the column was first set at 30°C for 7 min; then, with a ramp of 20°C/min, reached 100°C remaining at this temperature for 10 min. The injector and detector temperatures were 200 ºC and 300 ^{o}C, respectively.

The mixtures of cis-3-hexene and reference compounds with H_2O_2 were stable in the dark when left in the chamber for about 2h. The reaction of the organic species with H_2O_2 in the absence of UV light was of negligible importance over the typical time periods used in this work. No photolysis of either cis-3-hexene or the reference compounds was observed when mixtures of the reactants in the absence of H_2O_2 were irradiated for 30 min, using the output of all of the germicide lamps.

The reaction kinetics was followed by monitoring the decay of concentrations of the reactant and the reference compound, due to the reactions:

OH + cis-3-hexene→ products (Reaction 5, k_{hex})

OH + reference→ products (Reaction 6, k_{ref})

where, k_{hex} and k_{ref} are the rate coefficients for reactions of the cis-3-hexene and the reference compound with OH radicals, respectively. By assuming that the loss of cis-3-hexene and the reference compounds are only due to the reactions 5 and 6, the following expression can be adopted:

$$\ln\left(\frac{[\text{cis - 3 - hexene}]_0}{[\text{cis - 3 - hexene}]_t}\right) = \frac{k_{hex}}{k_{ref}} \times \ln\left(\frac{[\text{reference}]_0}{[\text{reference}]_t}\right) \quad \text{Equation 1}$$

where, the subscripts correspond to the time instants 0 and t, respectively.

The rate coefficient for the cis-3-hexene with OH radicals was measured at (298 ± 2) K and atmospheric pressure (750 ± 10) Torr, relative to the rate coefficients of the OH reactions with cyclohexene, 3-buten-1-ol and allyl ether, taken as reference compounds.

The initial concentrations used in the experiments were in the range of (8.36-14.51) × 10^{14} molecule cm^{-3} for the cis-3-hexene, (9.10-10.33) × 10^{14} molecule cm^{-3} for the cyclohexene, (8.61- 12.55) × 10^{14} molecule cm^{-3} for the 3-buten-1-ol and (17.47-24.85) × 10^{14} molecule cm^{-3} for the allyl ether. The concentration of H_2O_2 ranged from 41.82-54.12) × 10^{14} molecule cm^{-3}.

The chemicals used were cyclohexene (≥99 %. CAS: 110-83-8), 3-buten-1-ol (96%. CAS: 627-27-0) and allyl ether (98%. CAS: 557-40-4) supplied by Sigma-Aldrich. Cis-3-hexene (97%.CAS: 7642-09-3) was supplied by Alfa Aesar. He (99.999%. CAS: 7440-59-7) was supplied by Linde. H_2O_2 (70,5%. CAS: 7722-84-1) was supplied by

Atanor S.A. The organics were degassed by repeated freeze-pump-thaw cycling and purified by vacuum distillation before use.

3. Computational Methods

The cis-3-hexene + OH reaction has been described at Density Functional Theory (DFT) level, adopting the BHandHLYP functional[27] and the aug-cc-pVDZ basis sets.[28] This functional and basis set have been proven to give accurate results for this kind of reaction, performing as well as the *ab initio* CCSD(T) and QCISD(T) methods.[11] Geometry optimizations for all stationary points and saddle points have been performed and the characterization of these stationary points, after the successfully converged geometry optimization calculations, has been done by analysis of the vibrational frequencies, calculated at the same level.

The stationary points can be summarized as reactants, pre-barrier complex, saddle point and products. Spin contamination has been observed in all DFT calculations and in all cases the value has been greater than 0.750.

The minimum energy paths connecting the pre-barrier complex and product and passing through the saddle point have been calculated using the intrinsic reaction path (IRC) method.[29-31] For the description of the minimum energy path connecting the pre-barrier complex and the reactants, scan calculations have been performed by partially optimizing the geometries along a path of increasing C – OH interatomic distances. This procedure is appropriate for describing dissociation reactions with the further aim of

calculating rate coefficients.[32] Theoretical calculations have been performed with the Gaussian 09 program.[33]

Thermochemical quantities have been calculated using conventional Statistical Thermodynamics relations, assuming the harmonic oscillator, rigid rotor and ideal gas models, except for the case of the CH_3 internal rotations, which have been treated as hindered rotors.[34]

Microcanonical variational transition state rate coefficients,[35]over the temperature range 200-500 K have been calculated. The global rate coefficients (k_{global}) were calculated on the basis of the microcanonical variational rate coefficients obtained for each reaction step on the mechanism described above performed:

$$k_{global} = \sum_i x_i k_i$$ Equation 2

The subscript *i* stands for the conformers of cis-3-hexene and x_i are the populations of each conformer, calculated at each temperature as:

$$Pop_i(T) = \frac{\exp(-\Delta G_i(T)/RT)}{\sum \exp(-\Delta G_i(T)/RT)}$$ Equation 3

In fact, in our previous work, the adoption of the RRKM method has been proved to be very important for an accurate prediction of the rate coefficients.[11] The calculations are performed considering conservation of energy and angular momentum, for a range of energy values up to 50 kcal $mol^{-1}$and J values from 0 to 200. The sums of states for the outer and inner transition states ($N_1(E,J)$ and $N_2(E,J)$ (=$N_2^{(1)}(E,J)$ + $N_2^{(2)}(E,J)$, respectively) have been calculated by a variational procedure allowing the location of the microcanonical transition states along each reaction path using the RRKM code.[36] From $N_1(E,J)$ and $N_2(E,J)$, the effective sums of states are calculated as:[37]

$$\frac{1}{N_{eff}(E,J)} = \left(\frac{1}{N_1(E,J)} + \frac{1}{N_2(E,J)} \right)$$ Equation 4

This procedure is appropriate for the cases where that the steady state analysis, implemented at the canonical level, should not be appropriate for species as the pre-barrier complex. The energy and angular momentum constrains, however, must be respected and the dynamic description at the microcanonical level is recommended.[38] The high pressure rate coefficients have been finally calculated by the integral:

$$k^{\infty}(T) = \sigma_r \frac{1}{hQ_A Q_{OH} Q_{rel}} \int g_J N_{eff}(E,J) \exp\left(-\frac{E}{k_B T} \right) dJdE$$ Equation 5

where, σ_r, g_J, Q_A, Q_{OH} and Q_{rel} are the reaction path degeneracy, the degeneracy of the rotational states and the partition function for the unsaturated compound, A, for the OH and the relative translational partition function. The Planck and Boltzmann constants are conventionally represented by h and k_B. In all rate coefficients calculations, the spin-orbit effect for the OH radical has been considered.

4. Results and Discussion

4.1 Experimental Measurement of the Rate Coefficient

The bimolecular rate coefficient for the cis-3-hexene+ OH radical reaction, was measured, relative to the rate coefficients of the reaction of OH radicals with reference compounds, at (298± 2) K and atmospheric pressure. The reference reactions are:

OH + cyclohexene → products (Reaction 7, k_{CH})

OH + 3-buten-1-ol → products (Reaction 8, k_{31BO})

OH + allyl ether → products (Reaction 9, k_{AE})

where, k_{CH}, k_{31BO} and k_{AE} are the rate coefficients for the reference compounds (generally referred as k_{ref} and given in cm^3 $molecule^{-1}$ s^{-1}) measured by Atkinson et al.,[39] Cometto et al.[10] and Peirone et al.[40] as: $k_{CH} = (67.4 \pm 1.7) \times 10^{-12}$, $k_{31BO} = (5.7 \pm 0.1) \times 10^{-11}$ and $k_{AE} = (6.8 \pm 0.7) \times 10^{-11}$, respectively. At least, two experiments with each reference compound were performed, and the initial concentrations were varied in each experiment.

Figure 1 shows the $\ln([\text{cis-3-hexene}]_0/[\text{cis-3-hexene}]_t)$ as a function of the $\ln([\text{reference}]_0/[\text{reference}]_t)$, obtained for cyclohexene as the reference compound (the other curves, obtained with allyl ether and 3-buten-1-ol follow the same behaviour and are available as Electronic Supplementary Information). Significant linear correlation is observed in the experiments, with the R^2 value greater than 0.99. Moreover, the linear coefficients are close to zero, suggesting that the contribution of secondary reactions of the volatile organic compounds can be neglected. The initial concentrations of cis-3-hexene and of the reference compounds are presented in Table 1, as well as the number of experiments, the k_{hex}/k_{ref} ratio and the k_{ref} rate coefficient.

The estimated errors on the rate coefficients are propagated errors on the basis of the standard error of the slopes of the logarithm concentration curves and the error reported for the reference rate coefficients. In this approach, any systematic error due to sample handling and the chromatographic method are included in the dispersion of the

experimental curves and, therefore, in the standard error of the slope. The propagation of uncertainties of the independent variables follows the variance formula:[41]

$$(\delta_{k_{hex}})^2 = (\delta_{k_{ref}})^2 + (\delta_{\alpha})^2 \qquad \text{Equation 6}$$

where, $(\delta_{k_{ref}})^2$ and $(\delta_{\alpha})^2$ are the variances relative to the independent variables k_{ref} and the slope α, expressed as:

$$(\delta_i)^2 = \left[\left(\frac{\partial k_{hex}}{\partial i}\right)\delta_i\right]^2 \qquad \text{Equation 7}$$

for each independent variable i, and $(\delta_{k_{hex}})^2$ is the propagated uncertainty relative to the determined rate coefficient. The square root of the variance is the error associated with the independent variable i or to the measured rate coefficient. Since the k_{hex} rate coefficient was determined by at least two experiments with three reference compounds, the final reported rate coefficient is a mean value obtained from all the experiments and the uncertainty is chosen as the most restrictive value.

The rate coefficients obtained from the experiments with the three reference compounds showed negligible dispersion, 0.627×10^{-10} cm^3 molecule^{-1} s^{-1} being the mean value with 1.7% relative deviation. The error is mainly due, as discussed above, to the contributions of the uncertainty on the reference rate coefficient and the slope of the logarithm curve. The smallest uncertainty is achieved using cyclohexene as the reference compound, for which the relative uncertainties $(\delta_{k_{ref}} / k_{ref})$ and $(\delta_{\alpha} / \alpha)$ are 2.5% and 1.7% giving $(\delta_{k_{hex}} / k_{hex})$ as 3.0% and the uncertainty value, $\delta_{k_{hex}}$, as

0.019×10^{-10} cm^3 molecule $^{-1}$ s^{-1}. The corresponding relative uncertainties found on the determination of the rate coefficient using allyl ether and 3-buten-1-ol as the reference compounds are: 10.3% and 1.8% ($(\delta_{k_{ref}} / k_{ref})$, allyl ether and 3-buten-1-ol, respectively) and 2.4% and 9.5% ((δ_α / α), allyl ether and 3-buten-1-ol, respectively), yielding for each reference compound the uncertainty values : 0.066×10^{-10} and 0.060×10^{-10} cm^3 molecule $^{-1}$ s^{-1} (allyl ether and 3-buten-1-ol, respectively). Therefore, using cyclohexene as the reference compound, the experimental curves and the reference rate coefficient contribute similarly to the uncertainty of the measured rate coefficient, whereas with the allyl ether most of the uncertainty is due to reference rate coefficient and with the 3-buten-1-ol, to the experimental curve. Nevertheless, the three reference compounds were satisfactory for the determination of the rate coefficient for the cis-3-hexene + OH reaction and the final recommended value is $(6.27 \pm 0.66) \times 10^{-11}$ cm^3 molecule^{-1} s^{-1}. The final value is yet in agreement with the value 6.3×10^{-11} cm^3 molecule $^{-1}$ s^{-1}, previously estimated from structure-reactivity relations. [9]

4.2 Theoretical Model

The important structural and energetic aspects of the cis-3-hexene + OH reaction obtained at the BHandHLYP/aug-cc-pVDZ levels will be discussed in this section. The geometry of the cis-3-hexene was first located at the BHandHLYP/cc-pVDZ level and further refined by the addition of diffuse functions to the basis set. Before performing the new geometry optimization procedures, and in order to confirm that the starting structure of the cis-3-hexene is related to the global minimum geometry, scan calculations were performed over the dihedral angles, at the BHandHLYP/cc-pVDZ level, and the structures suggested from the scan calculation as local minimum energy

geometries, were further optimised at the BHandHLYP/aug-cc-pVDZ level. Vibrational frequencies calculations were also performed at the latter theoretical level, in order to characterize the stationary points. Two conformations of the reactant were located, as shown in Figure 2 (reactants *a* and *b*). The conformer *a* contributes with 48,3% of the population at 298K at the BHandHLYP/aug-cc-pVDZ level.

The energy difference, corrected by zero point vibrational energy, between the conformers *a* and *b* is 0.04 kcal mol^{-1} at the BHandHLYP/aug-cc-pVDZ level. The main differences between the two conformers are the dihedral angles $d_{H6C3C7C8}$ and $d_{H5C2C1C13}$. The conformer *a* shows the dihedral angles $d_{H6C3C7C8}$=58.55º and $d_{H5C2C1C13}$=58.52º on the other hand the conformer *b* shows the dihedral angles $d_{H6C3C7C8}$=55.63º and $d_{H5C2C1C13}$=-55.49º.

Literature strongly suggests that a pre-barrier complex plays an important role in the dynamics of the OH addition to unsaturated compounds.[21-23] Hence, starting with the two conformers, new calculations were performed with the aim of searching for possible geometries of pre-barrier complexes, related to each initial conformation of cis-3-hexene, and characterized as π-type (π-PC). Due to symmetry, the pre-barrier complexes resulting from the OH upward and downward attacks to conformer *b* are indistinguishable, therefore three distinct pre-barrier complexes were located (π-PC*c*, π-PC*d* and π-PC*e*). The relative energies, corrected by zero point vibrational energy, are shown in Table 2.

The three pre-barrier complexes show, at the BHandHLYP/aug-cc-pVDZ level, almost the same energy value, being located at 2.24 kcal mol^{-1}, below the reactants. The π-PC*c*,

π-PC*d* and π-PC*e* show the hydrogen atom of the OH radical oriented to the allylic plane, with dihedral angles $d_{O(OH)C3C2C1}$ = 90.33° , $d_{O(OH)C3C2C1}$ =88.81° and $d_{O(OH)C3C2C1}$ =96.91°, respectively. The oxygen-carbon bond distances are 2.50 Å ($O^{(OH)}$—C2) and 2.37 Å ($O^{(OH)}$—C3) for the π-PC*c*, 2.41 Å ($O^{(OH)}$—C2) and 2.41 Å ($O^{(OH)}$—C3) for the π-PC*d* and 2.46 Å ($O^{(OH)}$—C2) and 2.46 Å ($O^{(OH)}$—C3) for π-PC*e*.

No significant changes are verified for the C2C3 double bond distance or OH (from the alkene) at the π-PC with respect to that at the cis-3-hexene, being the C2C3 double bond distance 1.33 Å at the isolated alkene and 1.33 Å at the π-PC and the OH bond distance 0.97 Å at the isolated alkene and 0.97 Å at the π-PC.

The reaction profiles connecting the pre-barrier complexes to the isolated reactants were described by potential curves in which, starting from each π-PC, the $O^{(OH)}$—C2 distances were increased up to 10 Å, leading to the isolated reactants. At this point, the final energy observed on the potential curve showed reasonable agreement with the sum of the electronic energies of the isolated reactants.

Differently from the case of the pre-barrier complexes, the π interaction is not observed at the saddle points and only σ-type structures were located. Due to symmetry, the saddle points resulting from the OH upward and downward attacks are indistinguishable and four saddle points (TS*f*, TS*g*, TS*h* and TS*i*) were located, all above the corresponding π-PCs, but below the isolated reactants, stabilized by 0.61 kcal mol^{-1}, 0.69 kcal mol^{-1},0.45 kcal mol^{-1} and 0.80 kcal mol^{-1}, respectively. All saddle points could be well characterized by their imaginary frequencies.

The O – C interatomic distances are 2.61 Å (O – C2) and 2.23 Å (O – C3) at the TS*f*, 2.64 Å (O – C2) and 2.21 Å (O – C3) at the TS*g*, 2.64 Å (O – C2) and 2.20 Å (O – C3) at the TS*h* and 2.60 Å (O – C2) and 2.22(O – C3) at the TS*i*. Another important geometric feature is found at the C2C3 double bond distance, which is increased at the saddle points with respect the optimized values at the conformers *a* and *b*, being nearly 1.35 Å at all saddle points.

Starting from the saddle points, minimum energy paths were calculated by the IRC computational procedure. The resulting reaction paths clearly show the OH radical approaching the double bond and the O – C distances smoothly decreasing along the reaction coordinate, as expected for the OH addition to the carbon atoms at the double bond. The reaction paths lead to the formation of four radicals resulting from the addition of the hydroxyl radical to carbon atoms, yielding the radicals hereafter referred as PROD*j*, PROD*l*, PROD*m* and PROD*n*, from upward and downward attacks. The optimized geometries for each product conformation were obtained, being located 26.68, 26.47, 26.43 and 26.64 kcal mol^{-1}, respectively, below the isolated reactants.

The structures for reactants, pre-barrier complexes, saddle points and products are shown in Figure 2. The most relevant geometric parameters obtained at the BHandHLYP level with aug-cc-pVDZ basis sets are given as supplementary material.

The reaction mechanism is summarized as follows. The OH addition to conformer *a* results into the π-PC*c* pre-barrier complex, which further converts to the PROD*j* and PROD*l* products passing through the TS*f* and TS*g* saddle points. No significant distinction can be observed between the relative energies of the upward or downward

saddle points, suggesting competitive channels. The OH upward addition to conformer *b* results in the π-PC*d* pre-barrier complex, which then goes through the TS*h* saddle point along the reaction profile, converting into PROD*m*. The OH downward addition to conformer *b* results in the π-PC*e* pre-barrier complex, and TS*i* saddle point, finally reaching PROD*n*. The pre-barrier complexes show almost the same relative energies. No significant differences are found for the relative energies obtained for the TS*f* and TS*g* saddle points. Moreover, these relative energies are also similar to the relative energies obtained for the TS*h* and TS*i* saddle points and one cannot expect any prevalence for a particular addition channel.

4.3 Theoretical Rate Coefficients for the cis-3-hexene + OH Reaction

Rate coefficients were calculated for the association steps and dissociations and addition reactions of the PCc, PCd and PCe, represented by the detailed chemical model:

conformer a + OH →PCc	(Reaction 10, k_{1a})
PCc→ conformer a + OH	(Reaction 11, k_{-1a})
PCc→PRODj	(Reaction 12, $k_{2a}^{(1)}$)
PCc→PRODl	(Reaction 13, $k_{2a}^{(2)}$)
conformer b + OH →PCd	(Reaction 14, $k_{1b,up}$)
PCd→ conformer b + OH	(Reaction 15, $k_{-1b\ up}$)
PCd→PRODm	(Reaction 16, $k_{2b,up}$)
conformer b + OH →PCe	(Reaction 17, $k_{1b,down}$)

PCe→ conformer b + OH (Reaction 18, $k_{-1b,down}$)

PCe→PRODn (Reaction 19, $k_{2b,down}$)

The microcanonical variational rate coefficients (mCVT) were calculated and integrated as described above, using the theoretical molecular properties calculated at BHandHLYP level with aug-cc-pVDZ basis set.

A total of 20 geometries (and the corresponding molecular properties) along the potential curve representing the dissociation of the π-PCs (π-PCs → cis-3-hexene + OH) were used in order to evaluate the k_{-1a}, $k_{-1b,up}$ and $k_{-1b,down}$ rate coefficients. The $k_{1a,}$ $k_{1b,up}$ and $k_{1b,down,}$ rate coefficients were evaluated assuming the microscopic reversibility. For the calculation of the $k_{2a}^{(1)}$, $k_{2a}^{(2)}$, $k_{2b,up}$ and $k_{2b,down}$ rate coefficients, 21 points along the reaction coordinates (and the corresponding molecular properties) were used for the variational procedure.

Table 3 introduces the resulting rate coefficients in the range 200 – 500K, where k_{trans} corresponds to rate coefficients of the reaction with conformer *a* and k_{cis} corresponds to rate coefficients of the reaction with conformer *b*. At 298 K, the calculated rate coefficient obtained was 8.10×10^{-11} cm^3 $molecule^{-1}$ s^{-1}.

In these theoretical calculations, only the addition channel was considered. For the comparison of the calculated and experimental values, it should be noted that the experimental rate coefficient, $(6.27 \pm 0.66) \times 10^{-11}$ cm^3 $molecule^{-1}$ s^{-1}, is the sum of the addition and abstraction channels. Since the contribution of the abstraction channel has

not been valued, it may be inferred that the deviation between those values is at least 29%, which is a reasonable agreement.

Figure 3 shows the mCVT and experimental rate coefficients, represented in an Arrhenius plot. The calculated rate coefficients decrease as the temperature increases and follow the expression (the parameters are in units of cm^3 $molecule^{-1}$ s^{-1} and kJ mol^{-1}):

$$k(T) = 6.69x10^{-12} \exp\left(\frac{6.21}{RT}\right) \qquad \text{Equation 8}$$

4.4 Reactivity Aspects and Atmospheric Implications

In order to evaluate the predicted rate coefficients for the OH + cis-3-hexene reaction, a comparative analysis of the reactivity of a series of alkenes towards OH radicals was done. Similar values are observed for the rate coefficients, at 296 ± 2 K, for the reactions of OH radicals with propene (3.0×10^{-11} cm^3 $molecule^{-1}$ s^{-1}),[42] 1-butene (3.1×10^{-11} cm^3 $molecule^{-1}$ s^{-1}), 1-pentene (3.1×10^{-11} cm^3 $molecule^{-1}$ s^{-1}) and 1-hexene (3.7×10^{-11} cm^3 $molecule^{-1}$ s^{-1}).[43] The addition of alkyl groups along the carbon chain apparently does not interfere in the rate coefficient when the double bond is at the terminal carbon atom. Nevertheless, an increase of the rate coefficients is observed upon substitution of the hydrogen atom connected to carbon atoms at the double bond. When the rate coefficients for the reactions of OH radicals with cis-2-butene (5.6×10^{-11} cm^3 $molecule^{-1}$ s^{-1})[43] or cis-2-pentene (6.5×10^{-11} cm^3 $molecule^{-1}$ s^{-1})[43] are compared with reactions of OH radicals + propene, or any other compound in that group, the values

increase almost twice. The increase of the rate coefficients may be due to the replacement of H atoms by the electron donating alkyl group.

The compounds cis-2-butene and cis-3-hexene have similar carbon chains, with two H atoms and two alkyl groups attached to the double bond carbon atoms, and are expected to show similar reactivity towards OH radicals. Thus, the rate coefficients must be, at least, very close. In fact, our experimental rate coefficient value for the cis-3-hexene + OH reaction deviates 12% from the rate coefficient, at 298 K, for the cis-2-butene + OH reaction. This is in reasonable agreement with previous works, [10,17] which suggest that the dependence of the rate coefficients with the carbon numbers of the aliphatic structure seems to be very weak, unless the structure presents a substituent group on the double bond carbon atom, leading to an increase in the rate coefficients values. Similar analysis is done for the predicted cis-3-hexene + OH rate coefficients and the experimental cis-2-butene + OH rate coefficients at the range from 300 – 450 K. Figure 4 compares the theoretical values obtained for the cis-3-hexene + OH addition reaction and the experimental rate coefficients for the cis-2-butene + OH reaction, obtained by Atkinson et al.[43] **Error! Bookmark not defined.** Besides the similarity between the experimental rate coefficients for the cis-2-butene + OH and cis-3-hexene + OH reactions, at 298 K, the theoretical rate coefficient for the cis-3-hexene + OH reaction also agree with the experimental rate coefficients for the cis-2-butene + OH reaction, over this temperature range, as can be seen from Figure 4. The theoretical and experimental rate coefficients deviate less than 25%.

Another significant comparison should be done, and refers to the study of the reactivity of alkenes and unsaturated alcohols with the same aliphatic structure. In a comparative

study of the reactivity of unsaturated alcohols and alkenes analogues, towards OH radicals, at the same temperature, Cometto et al.,[10] indicated that the rate coefficients for the OH addition to unsaturated alcohols show higher values, suggesting that the substitution of a hydrogen atom by a OH group increase the reactivity. The substitution factor, defined as k(OH)/k(H), was shown to vary from 1.7 to 2.5. The experimental rate coefficient value, at 298 K, for the reaction of cis-3-hexen-1-ol with OH radicals (1.4×10^{-10} cm^3 $molecule^{-1}$ s^{-1}) was obtained for Gibilisco et al.,[17] and is 2.2 times higher than our experimental value for cis-3-hexene, in a good agreement with the substitution factor suggested by Cometto et al.[10] The increased reactivity of the unsaturated alcohols towards OH radicals, in respect to the alkene analogue, has been suggested to be due to the hydrogen bonds stabilizing the π-PC and saddle points.[11] From the comparison of the rate coefficients for the cis-3-hexen-1-ol + OH[16] and and cis-3-hexene + OH addition reactions it can be noted the unsaturated alcohol reacts with OH radicals faster than the alkene, over the temperature range 250-350 K, for which the experimental values for the cis-3-hexen-1-ol reaction have been determined, and considering only the addition channel for the cis-3-hexene + OH reaction.

Besides the reaction of cis-3-hexene with OH radicals, it is worthy of noticing the reactivity towards O_3 and NO_3, two other possible removal channels of this alkene from the troposphere. The effective lifetimes of cis-3-hexene with respect the reaction with each oxidant were calculated using the relationship:

$$\tau_X = \frac{1}{k_X[X]} \qquad \text{Equation 9}$$

with X = OH and NO_3 radicals and O_3 molecules and using the 12 h average day-time global concentration of OH radicals of 1×10^6 radicals cm^{-3}, the 12 h average night-time concentration of NO_3 of 5×10^8 mol cm^{-3} and 24 h average O_3 concentration of 7×10^{11} molecule cm^{-3}.[44-46] The estimated lifetimes due to depletion of cis-3-hexene by OH and NO_3 radicals and ozone are 4.43, 1.27 and 2.75 hours, respectively. These estimated values do not take account local atmospheric conditions and different seasons which are capable to change these oxidant concentrations. The lifetime data indicate that the cis-3-hexene is rapidly removed in the gas phase by these oxidants, suggesting that this compound will be degraded near its emission sources.

5. Conclusions

In this work, the mechanism and rate coefficients for the OH addition to cis-3-hexene have been investigated in detail, for the first time, by both experimental and theoretical methods. The room temperature rate coefficient for the reactions of OH radicals with cis-3-hexene has been obtained using the relative rate method. Moreover, on the basis of BHandHLYP/aug-cc-pVDZ and variational microcanonical transition state calculations, theoretical rate coefficients have been predicted in the range 200 – 500K.

The rate coefficients, obtained from the experiments with the three reference compounds (allyl ether, 3-buten-1-ol and cyclohexene), showed negligible dispersion among the determinations (1.7%). Our final recommended value is $(6.27 \pm 0.66) \times 10^{-11}$ cm^3 molecule $^{-1}$ s^{-1}.

The calculated rate coefficient for the cis-3-hexene + OH reaction at 298 K, adopting the microcanonical variational transition state method, was 8.10×10^{-11} cm^3 $molecule^{-1}$ s^{-1} at the BHandHLYP/aug-cc-pVDZ level, in good agreement with the experimental value. Moreover the dependence on the temperature agrees with the reaction of OH radical with the cis-2-butene, in the temperature range 300-450K.

The comparison between the experimental rate coefficient for the cis-2-butene + OH radicals (5.6×10^{-11} cm^3 $molecule^{-1}$ s^{-1}) and our experimental rate coefficient for the cis-3-hexene + OH radicals reaction, at 298K, indicated that our result is in a good agreement with the literature, since compounds with similar carbon chains should show similar reactivity towards OH radicals. The ratios of the rate coefficients for the reaction of cis-3-hexene and cis-3-hexen-1-ol with OH radicals have also been investigated as a function of the temperature, suggesting that at room temperature the cis-3-hexen-1-ol reacts with the OH radicals faster than cis-3-hexene, by a factor of 2.2.

Our results suggest that the theoretical mechanism, based on DFT calculations, using the microcanonical variational transition state method is satisfactory for understanding the experimental results, to clarify the experimental observations and to model the reaction kinetics and dynamics, the good agreement of the experimental data with the theoretical results, contributes significantly to the validation of the theoretical methodology for calculating rate coefficients for reactions of alkenes with OH radicals.

Acknowledgments.

The authors thank the Brazilian National Council for Scientific and Technological Development, CNPq (PROSUL, Proc. 490252/2011-7) and CONICET, ANPCyT-FONCyT, MinCyT and SECyT-UNC of Argentina for financial support of this research.

Figure Captions

Figure 1: Plot of the kinetic data for the reaction of cis-3-hexene with OH radicals using cyclohexene as reference compound. $[S]_0$ and $[S]_t$ are the concentrations of the cis-3-hexene at times 0 and t, respectively, $[R]_0$ and $[R]_t$ are the concentrations of the reference compound at times 0 and t, respectively.

Figure 2: The structures for reactants, pre-barrier complex, saddle points and products along the cis-3-hexene +OH reaction profile.

Figure 3: Microcanonical variational rate coefficients (mCVT) and experimental rate coefficients (cm^3 $molecule^{-1}$ s^{-1}), as a function of the temperature (K). The theoretical rate coefficients were calculated on the basis of the BHandHLYP/aug-cc-pVDZ data.
Figure 4: Rate coefficients (cm^3 $molecule^{-1}$ s^{-1}) for the reactions of OH radicals with cis-2-butene and with cis-3-hexene as a function of the temperature (K).

Tables

Table 1. Initial concentration of the reactants (HEX: cis-3-hexene and REF: reference compound, in ppm), rate constant ratios, $k_{HEX}/k_{REF,}$ and the relative rate constants, k_{HEX}, for the reaction of OH radicals with cis-3-hexene at 298 K and atmospheric pressure.

Reference compound	Run	$[REF]_0$ ppm	$[HEX]_0$ ppm	k_{HEF}/k_{REF}	k_{HEX} cm^{-3} $molecule^{-1}$ s^{-1}
cyclohexene	1	42.28	34.55	0.950±0.016	$(6.41\pm0.19)\times10^{-10}$
	2	36.24	49.51	0.9106±0.016	$(6.14\pm 0.19)\times10^{-10}$
3-buten-1-ol	1	35.20	58.20	1.099±0.104	$(6.26\pm0.60)\times10^{-11}$
	2	50.10	52.90	1.099±0.087	$(6.27\pm0.51)\times10^{-11}$
allyl ether	1	71.60	52.40	0.914±0.022	$(6.21\pm0.66)\times10^{-11}$
	2	100.20	59.00	0.928±0.016	$(6.31\pm0.66)\times10^{-11}$
			Average		**$(6.27\pm0.66)\times10^{-11}$**

Tables

Table 2.Relative total energies (ΔE, in kcal mol^{-1}) and relative energies including zero-point vibrational energy corrections (ΔE^0, in kcal mol^{-1}) for the several stationary points involved in the OH + cis-3-hexene reaction, in relation to the isolated reactants (global minimum), calculated at the BHandHLYP /aug-cc-pVDZ level.

	ΔE (kcal mol^{-1})	**ΔE^0 (kcal mol^{-1})**
cis-3-hexene[a] + OH	0.00	0.00
π-PCc	-3.52	-2.19
TSf	-2.04	-0.61
TSg	-2.31	-0.69
PRODj	-30.21	-26.68
PRODl	-30.00	-26.47
cis-3-hexene[b] + OH	0.00	0.00
π-PCd	-3.52	-2.22
π-PCe	-3.51	-2.24
TSh	-2.06	-0.45
TSi	-2.31	-0.80
PRODm	-29.98	-26.43
PRODn	-30.19	-26.64

a: *trans* conformer

b: *cis* conformer

Tables

Table 3. Microcanonical variational rate coefficients, k_{global} (cm^3 $molecule^{-1}$ s^{-1}) calculated for the cis-3-hexene + OH reaction, as a function of the temperature.

Temperature (K)	k_{cis}	k_{trans}	k_{global}
200	1.33×10^{-10}	4.50×10^{-10}	2.83×10^{-10}
250	6.58×10^{-11}	2.04×10^{-10}	1.32×10^{-10}
300	4.12×10^{-11}	1.21×10^{-10}	7.96×10^{-11}
350	2.97×10^{-11}	8.32×10^{-11}	5.57×10^{-11}
400	2.35×10^{-11}	6.34×10^{-11}	4.29×10^{-11}
450	1.97×10^{-11}	5.16×10^{-11}	3.53×10^{-11}
500	1.74×10^{-11}	4.40×10^{-11}	3.04×10^{-11}

Figures

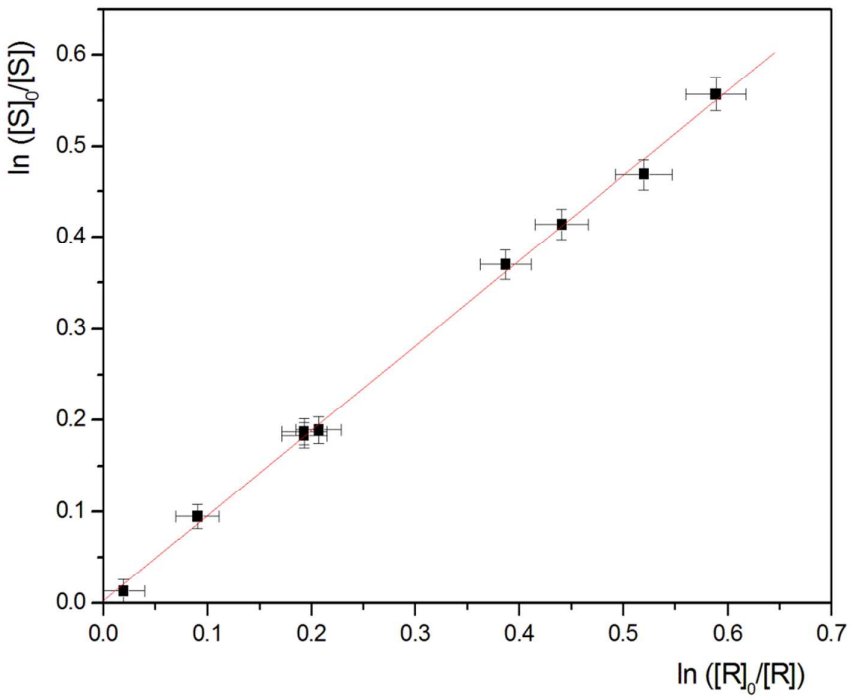

Figure 1. Plot of the kinetic data for the reaction of cis-3-hexene with OH radicals using allyl ether as reference compound. $[S]_0$ and $[S]_t$ are the concentrations of the cis-3-hexene at times 0 and t, respectively, $[R]_0$ and $[R]_t$ are the concentrations of the reference compound at times 0 and t, respectively.

Figures

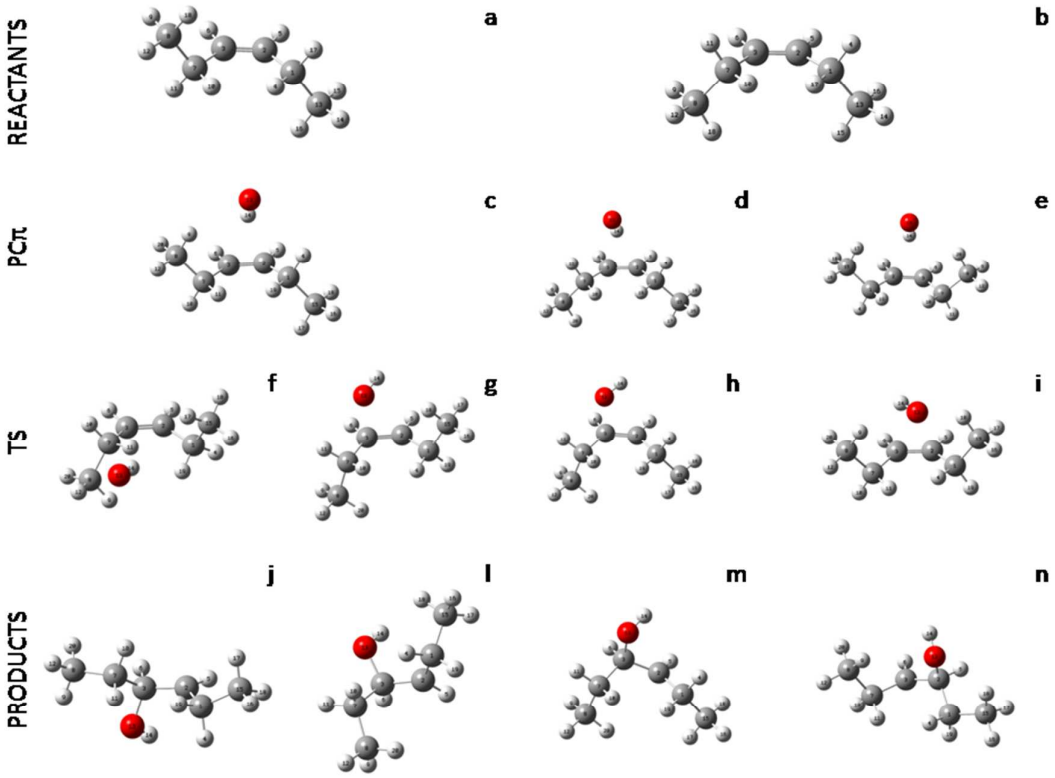

Figure 2. The structures for reactants, pre-barrier complex, saddle points and products along the cis-3-hexene +OH reaction profile.

Figures

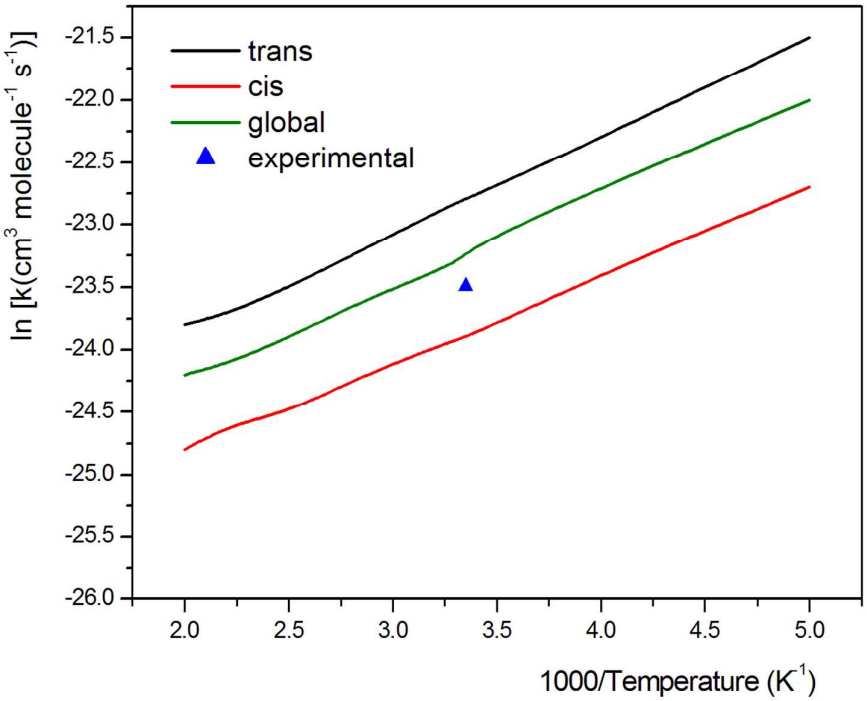

Figure 3. Microcanonical variational rate coefficients (mCVT) and experimental rate coefficients (cm^3 $molecule^{-1}$ s^{-1}), as a function of the temperature (K). The theoretical rate coefficients were calculated on the basis of the BHandHLYP/aug-cc-pVDZ data.

Figures

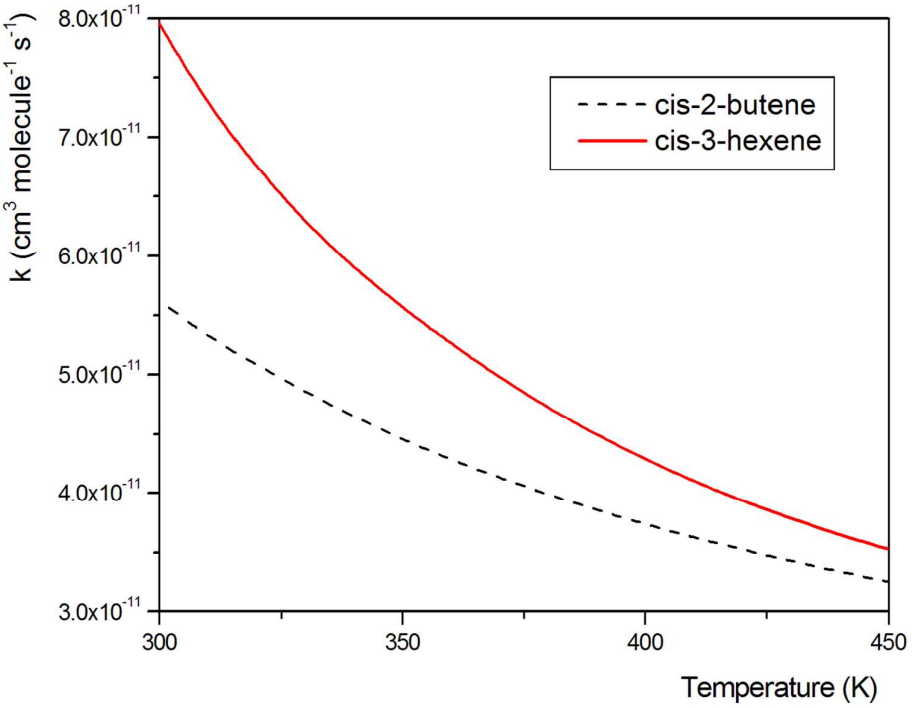

Figure 4. Rate coefficients (cm^3 $molecule^{-1}$ s^{-1}) for the reactions of OH radicals with cis-2-butene and with cis-3-hexene as a function of the temperature (K).

References

1 A. B. Guenther, X. Jiang, C. L. Heald, T. Sakulyanontvittaya, T. Duhl, L. K. Emmons and X. Wang, *Geosci. Model Dev.,* 2012, **5**, 1471.

2 R. Atkinson, *Atmos. Environ.*, 2000, **34**, 2063.

3 B. J. Finlayson-Pitts and J. N. Pitts, Jr., *Chemistry of the Upper and Lower Atmosphere*. Academic Press, San Diego, California, 2000.

4 B. Yuan, W. W. Hu, M. Shao, M. Wang, W. T. Chen, S. H. Lu, L. M. Zeng and M. Hu, *Atmos. Chem. Phys*., 2013, **13**, 8815.

5 O. Ramnäs, U. Östermark and G. Petersson, *J. Chromatogr. A,* 1993,638, 65.

6 J. S. Heath, K. Koblis and S. L. Sager, *J. Soil Contam.*, 1993, 2, 1.

7 J. G. Calvert, R. Atkinson, J. A. Kerr, S. Madronich, G. K. Moortgat, T. J. Wallington and G. Yarwood, *The Mechanisms of Atmospheric Oxidation of the Alkenes*; Oxford University Press, Inc., New York, 2000.

8 C. Pfrang, R. S. Martin, A. Nalty, R. Waring, C. E. Canosa-Mas and R. P. Wayne, *Phys. Chem. Chem. Phys.*, 2005, **7**, 2506.

9 D. Grosjean and E. L. Williams II, *Atmos. Environ.*, 1992, **26**, 1395.

10 P. M. Cometto, P. R. Dalmasso, R. A. Taccone, S. I. Lane, F. Oussar, V. Daële, A. Mellouki and G. Le Bras, *J. Phys. Chem. A*, 2008, **112**, 4444.

11 T. S. Barbosa, J. D. Nieto, P. M. Cometto, S. I. Lane, G. F. Bauerfeldt and G. Arbilla, *RSC Adv*., 2014, **4**, 20830.

12 T. D. Sharkey, *Trend plant sci.,* 1996, **1**, 78.

13 A. Hatanaka, *Phytochem.,* 1993, **34**, 1201.

14 R. Atkinson, J. Arey, S. M. Aschmann, S. B., Corchnoy and Y. Shu, Y., *Int. J. Chem. Kinet.*, 1995, **27**, 941.

15 E. Jimenez, B. Lanza, M. Antiñolo and J. Albaladejo, *Environ. Sci. Technol.,* 2009, **43**, 1831.

16 M. E. Davis and J. B. Burkholder, *Atmos. Chem. Phys. Discuss.*, 2011, **11**, 2377.

17 R. G. Gibilisco, A. N. Santiago and M. A. Teruel, *Atmos. Environ.,* 2013, **77**, 358.

18 W. Zhang, B. Du and C. Feng, *Theor. Chem. Acc.*, 2010, **125**, 45

19 M. C. Piqueras, R. Crespo, I. Nebot-Gil and F. Tomás, *J. Mol. Struc-Theochem*., 2001, **537**, 199.

20 M. Francisco-Márquez, J. R. Alvarez-Idaboy, A. Galano and A. Vivier-Bunge, *Phys. Chem. Chem. Phys.*, 2004, **6**, 2237.

21 D. L. Singleton and R. J. Cvetanovic, *J. Am. Chem. Soc*., 1976, **98**, 6812.

22 R. J. Cvetanovic, *J. Chem. Phys.*, 1960, **33**, 1063.

23D. V. Banthorpe, *Chem. Rev*., 1970,**70**,295

24 P. R. Dalmasso, R. A. Taccone, J. D. Nieto, M. A. Teruel and S. I. Lane, *Atmos. Environ*., 2006, **40**, 7298.

25 P. R. Dalmasso, R. A. Taccone, J. D. Nieto, P. M. Cometto and S. I. Lane, *Atmos. Environ.*, 2010, **44**, 1749.

26 J. P. A. Abrate, I. Pisso, S. A. Peirone, P. M. Cometto and S. I. Lane, *Atmos. Environ*., 2013,**67**, 85.

27 A. D. Becke, *J. Chem. Phys.*, 1993, **98**, 1372.

28 T. H. Dunning, *J. Chem. Phys.*, 1989, **90**,1007.

29. K. A. Fukui, *J. Phys. Chem*., 1970, **74**, 4161

30 C. Gonzales and H. B. Schelegel, *J. Chem. Phys*., 1989, **90**, 2154.

31 C. Gonzales and H. B. Schelegel, *J. Chem. Phys*., 1990, **94**, 5523.

32 R. C. M. Oliveira and G. F. Bauerfeldt, *Int. J. Quant. Chem.*, 2012, **112**, 3132.

33 M. J. Frisch, G. W. Trucks, H. B. Schlegel, G. E. Scuseria, M. A. Robb, J. R Cheeseman, G. Scalmani, V. Barone, B. Mennucci, G. A. Petersson, H. Nakatsuji, M. Caricato, X. Li, H. P. Hratchian, A. F. Izmaylov, J. Blondo, G. Zheng, J. L. Sonnenberg, M. Hada, M. Ehara, K. Toyota, R. Fukuda, J. Hadsegawa, M. Ishida, T. Nakajima, Y. Honda, O. Kitao, H. Nakai, T. Vreven, JR. J.A. Montgomery, J. E. Peralta, F. Ogliaro, M. Bearpark, J. J. Heyd, E. Brothers, K. N. Kund, V. N. Staroverov, R. Kobayashi, J. Normand, K. Raghavachari, A. Rendell, J. C. Burant, S. S. Iyengar, J. Tomasi, M. Cossi, N. Rega, J. M. Millam, M. Klene, J. E. Knox, J.B. Cross, V. Bakken, C. Adamo, J. Jaramillo, R. Gomperts, R. E. Stratmann, O. Yazyev, A.J. Austin, R. Cammi, C. Pomelli, J. W. Ochterski, R. L., Martin, K. Morokuma, V. G. Zakrzewski, G. A. Voth, P. Salvador, J. J. Dannenberg, S. Dapprich, A. D. Daniels, Ö. Farkas, J. B. Foresman, J. V. Ortiz, J. Cioslowski, D.J. Fox, *Gaussian09, (Revision A.02)*, Gaussian, Inc., Wallingford, CT, 2009.

34 C. J. Cramer, *Essentials of Computational Chemistry Theories and Models*. Wiley, Hoboken, 2004.

35J.I. Steinfeld, J.S. Francisco and W.L. Hase, *Chemical Kinectics and Dynamics*, Upper Saddle River, New Jersey, 1999.

36 L. Zhu and W. L. Hase, *Chem. Phys. Lett*.,1990, **175**, 117.

37 W. H. Miller, *J. Chem. Phys*., 1976, **65**, 2216.

38 E. E. Greenwald, S. W. North, Y. Georgievskii and S. J. Klippenstein, *J. Phys. Chem. A*, 2005, **109**, 6031.

39 R. Atkinson, S.M. Aschmann and W.P.L. Carter*, Int. J. Chem. Kinet*., 1983, **15**, 1161.

40 S.A. Peirone, J. P. A. Abrate, R. A. Taccone, P. M. Cometto and S. I. Lane, *Atmos. Environ.,* 2011, **45**, 5325.

41 H. H. Ku, *J. Res. Natl. Stand.*, 1966, **70C**, 263.

42 O. J. Nielsen, O. Jørgensen, M. Donlon, H. W. Sidebottom, D. J. O'Farrell and J. Treacy, *Chem. Phys. Lett*., 1990, **168**, 319.

43 R. Atkinson, *Chem. Rev*., 1986, 86, 69.

44 R. G. Prinn, J. Huang, R. F. Weiss, D. M. Cunnold, P. J. Fraser, P. G. Simmonds, A. McCulloch, C. Harth, P. Salameh, S. O'Doherty, R. H. J. Wang, L. Porter and B. R. Miller, *Science*, 2001, **292**, 1882.

45 Y. Shu and R. Atkinson, *J. Geophys. Res.,* 1995, ***100*****,** 7275.

46 J. A. Logan, *J. Geophys. Res*. 1985, **90**, 10463.